Title

Ion-capture electrodialysis using multifunctional adsorptive membranes

Journal

Science, 372(6539)

ISSN

0036-8075

Authors

Uliana, Adam A

Bui, Ngoc T

Kamcev, Jovan

et al.

Publication Date

2021-04-16

DOI

10.1126/science.abf5991

Peer reviewed

Title: Ion-capture electrodialysis by multifunctional porous aromatic framework adsorbent membranes

Authors: Adam A. Uliana,[1,2] Ngoc T. Bui,[3,†] Jovan Kamcev,[4,‡] Mercedes K. Taylor,[4,§] Jeffrey J. Urban,[3] Jeffrey R. Long[1,2,4,*]

Affiliations:

[1]Department of Chemical and Biomolecular Engineering, University of California, Berkeley, CA 94720, United States.

[2]Materials Sciences Division, Lawrence Berkeley National Laboratory, Berkeley, CA 94720, United States.

[3]The Molecular Foundry, Lawrence Berkeley National Laboratory, Berkeley, CA 94720, United States.

[4]Department of Chemistry, University of California, Berkeley, CA 94720, United States.

*Correspondence to: jrlong@berkeley.edu.

[†]Present address: School of Chemical, Biological, and Materials Engineering and School of Civil Engineering and Environmental Science, University of Oklahoma, Norman, OK 73019, United States.

[‡]Present address: Department of Chemical Engineering, University of Michigan, Ann Arbor, MI 48109, United States.

[§]Present address: Department of Chemistry and Biochemistry, University of Maryland, College Park, MD 20742, United States.

Abstract: Technologies that can efficiently purify nontraditional water sources are urgently needed to meet the rising global demands for clean water. Water treatment plants typically require a series of costly separation units to achieve desalination and the challenging removal of trace contaminants (e.g., heavy metals, boron) from these complex waters. We report a new separation strategy coined "ion-capture electrodialysis" that, for the first time in an efficient one-unit process, can desalinate practically any water source while simultaneously recovering targeted solutes with near-perfect selectivity. Electrodialysis membranes embedded with porous aromatic framework adsorbents developed for this separation exhibit new properties useful for general electrochemical applications and can be easily tuned to selectively capture virtually any contaminant. Principles established herein can also be applied broadly to existing membrane processes to originate other unprecedently efficient and selective multifunctional separations.

One Sentence Summary: A new class of tunable membranes are used to create one-step separations that can desalinate any water source while recovering targeted solutes with exceptional selectivity.

Main Text: The rapidly growing demands for water in agriculture, energy, industry, and municipal sectors necessitate the immediate expansion of sustainable clean water resources. Water stresses have caused conventional freshwater supplies to be diminishing at faster rates than can be replaced (*1*). Nontraditional water sources (e.g., wastewater, brackish water, seawater) could alternatively provide abundant water globally. However, these complex solutions contain high salt concentrations and trace yet toxic ionic contaminants (e.g., heavy metals, oxyanions, fluoride), which vary by location and type of water source (*2-4*). At the same time, nontraditional waters often contain high-value ions (e.g., uranyl in seawater, precious metals and nutrients in wastewater), but current technologies lack the efficiency and selectivity needed for their cost-effective extraction (*5, 6*). Electrodialysis and reverse osmosis are among the most common membrane-based technologies used for removing ions from water (*2, 4*). These approaches, however, are incapable of selectively isolating individual solutes, and toxic ions are instead returned to the environment with the concentrated brine solutions (*2*). Accordingly, developing membranes technologies with drastically improved selectivity for either water desalination or the recovery of individual molecules from water are considered as two of the greatest "holy grail" objectives in the separations industry (*3-5, 7, 8*).

We report an unprecedented multifunctional separation strategy that recovers target ions from water with near-perfect selectivity while simultaneously desalinating water for re-use. We coin this water purification process "ion-capture electrodialysis" ("IC-ED"). In this approach (Fig. 1A,B), adsorbent nanoparticles selective for targeted ions are blended into ion exchange membranes. These composite membranes are then placed in an electrodialysis setup, where an external electric field is applied to drive ions in a feed water stream through the membranes and toward the receiving streams. While target ions are selectively captured by adsorbents embedded in the membranes, competing ions (e.g., Na^+, Cl^-) permeate freely to desalinate the feed. In typical desalination plants, a series of energy-intensive pre- and post-treatment separation units are required to isolate components of interest from water (*9*). In comparison, IC-ED concurrently achieves three major benefits in an efficient one-step process: recovered target ions that can be re-used as high-value commodities or properly disposed as waste, desalinated and detoxified water, and obtained non-toxic brine streams that can be returned to the environment in a safer manner. In this report, we develop a new class of adsorptive membrane materials that can be easily altered to shift selectivity toward virtually any targeted solute, and we elucidate the promising potential of IC-ED processes through extensive adsorption, electrodialysis, and diffusion dialysis studies.

Adsorptive membranes are an emerging class of materials with improved separation performance compared to conventional membranes (*4, 10-14*). However, limited tunability, capacities, and selectivities remain major challenges in their development (*4*). We sought to transcend these limitations by developing membranes incorporated with porous aromatic framework (PAF) adsorbents in our IC-ED studies. PAFs possess a high-porosity, diamondoid-like structure composed of organic nodes covalently coupled to aromatic linkages (Fig. 1C) (*15*). Pore morphologies and chemical affinities optimal for specific adsorbates can be constructed through the rational choice of node, linker, and linker-appended chemical functionality (*16*). Indeed, functionalized PAF variants have been reported with among the highest selectivities, kinetic rate constants, and capacities in literature for capturing Hg^{2+} (*17*), Nd^{3+} (*18*), Cu^{2+} (*19*), Pb^{2+} (*20*), UO_2^{2+} (*21, 22*), $B(OH)_3$ (*23*), Fe^{3+} (*24*), or $AuCl_4^-$ (*25*) from water. Meanwhile, other highly tunable nanomaterial classes (e.g., metal–organic frameworks) often lack stability in water and compatibility with polymer matrices due to inorganic parts (*26*). PAFs conversely display exceptional hydrothermal stability and chemical compositions similar to those of polymer matrices (*16*). Few reports, however, have demonstrated PAF-incorporated membranes, with applications mostly limited to anti-aging gas separation membranes and thin-film composites (*16, 27*). PAF membranes originated herein exhibit many useful properties for new directions in IC-ED processes and general water treatment, electrochemical, and adsorptive membrane applications.

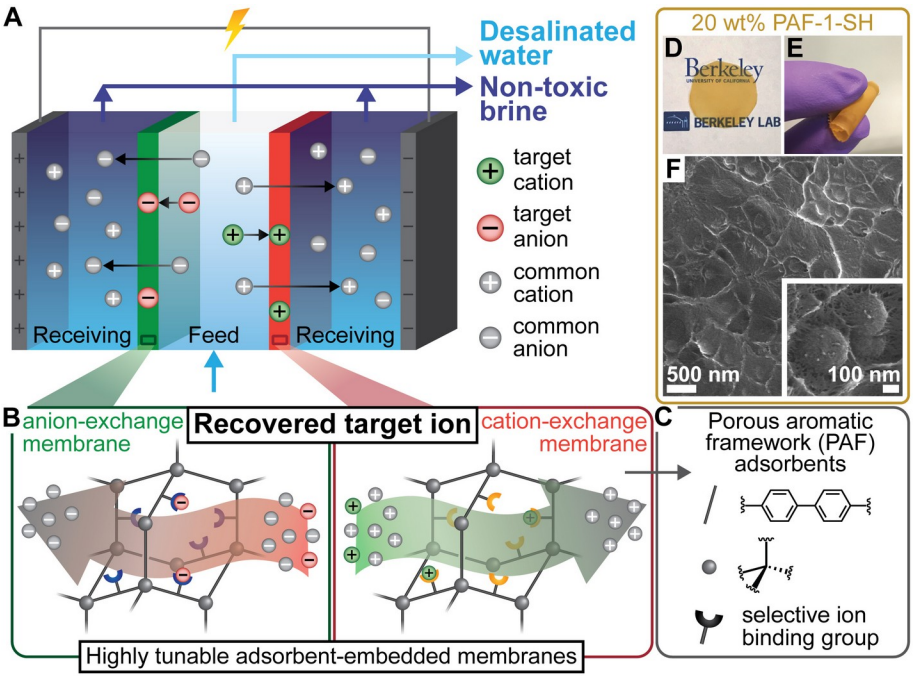

Fig. 1. Design of ion-capture electrodialysis (IC-ED) and tunable membranes. (A) Upon applying an external electric field to trigger ion migration across ion-exchange membranes, **(B)** target ions (e.g., Hg^{2+}) are selectively captured by adsorbents dispersed in the membranes. Simultaneously, common waterborne ions (e.g., Na^{+}) permeate across the membranes to desalinate the feed and generate non-toxic receiving solutions. The target ion is recovered for commodity re-use or proper disposal upon controlled release from the adsorbents. Though not shown, water splitting occurs at both electrodes to maintain electroneutrality. **(C)** In this work, high-performance, highly tunable porous aromatic frameworks (PAFs) with selective ion binding pore pockets are used as model adsorbents embedded in polymer matrices. PAF-embedded membranes exhibit **(D)** defect-free and optically transparent morphologies, indicating high PAF dispersibility, and **(E)** high flexibility optimal for ease in handling. **(F)** Cross-sectional scanning electron micrographs (zoom-in displayed in inset) also show high PAF dispersibility and strong, favorable interactions between the PAFs and polymer matrix.

Membranes consisting of up to 20 wt% of Hg^{2+}-selective PAF-1-SH (*17*) in a sulfonated polysulfone (sPSF) cation exchange matrix (figs. S1, S6, and S7) were fabricated and characterized as model PAF membranes. Notably, to our best knowledge, 20 wt% is the highest achieved PAF loading yet reported in composite membranes. Loadings were verified by thermogravimetric analysis (fig. S17 and table S2). High PAF dispersity in the films is indicated by their optical transparency (Fig. 1D and fig. S2), and PAF membranes can be easily bent and distorted without damage for ease in handling (Fig. 1E and fig. S3). Dynamic light scattering and scanning electron microscopy (SEM) images reveal that the PAFs are spherical with typical diameters of ~200 nm (figs. S15 and S16). These particles are observed uniformly without agglomerations, defects, or sieve-in-a-cage morphologies in cross-sectional SEM images of 20 wt% PAF-1-SH membranes (Fig. 1F and fig. S18). These observations confirm that PAF composite membranes are uniform and robust, likely due to favorable van der Waals forces

between the PAFs and polymer, π-π stacking between aromatic groups, and polymer pore plugging into PAF mesopores (*27*).

Conventional charged membranes face an ion permeability-selectivity tradeoff, where higher swelling decreases permselectivity but enlarges free volume pathways, leading to higher permeability and water uptake (*28*). However, PAF-incorporated membranes advantageously exhibit an inverse effect. While PAFs add porosity to the membranes to elevate water uptake and ion permeability, strong PAF-polymer crosslinking interactions diminish swelling (Fig. 2A). These interfacial interactions are observed abundantly in cross-sectional SEM images (Fig. 1F inset) and are corroborated by drastic increases in membrane glass transition temperature (T_g) upon increased PAF loadings (up to 19°C, Fig. 2B). To further probe dimensional and chemical stabilities of the PAF membranes, dissolution studies were performed by re-immersing membranes in casting solvents, 12 M HCl, or 12 M NaOH for 24 h. While neat sPSF membranes expectedly redissolved in casting solvents, crosslinking interactions were so abundant in 20 wt% PAF-1-SH membranes that they remained fully or partially insoluble in each solvent (fig. S20). Similarly, neat sPSF membranes with ultra-high charge densities become water-soluble due to excessive water uptake (figs. S6, S7, and S21). However, upon incorporation of PAFs into these matrices, crosslinking interactions enable water-stable PAF membranes to be fabricated (fig. S21, see Supplementary Text). These exciting findings suggest that PAF fillers may be applied generally to achieve charge densities, ion conductivities, and permeabilities higher than possible for neat membranes.

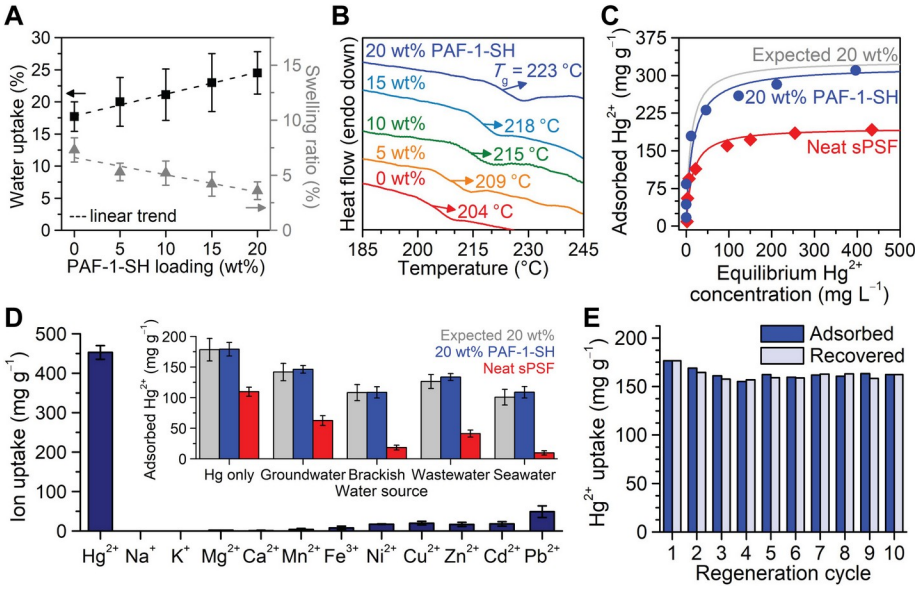

Fig. 2. Physical and adsorptive properties of PAF-embedded membranes. (A) Increased water uptake and swelling resistance in water by membranes with increased PAF loadings due to PAF pore accessibility and PAF-polymer crosslinking interactions, respectively. These favorable interactions are corroborated by **(B)** drastically elevated membrane glass transition temperature (T_g) with increased PAF loading. **(C)** Equilibrium Hg^{2+} adsorption isotherms of fabricated membranes. Solid lines represent Langmuir model fits. Expected 20 wt% (gray) data are the theoretical Hg^{2+} uptake when all PAFs in membranes are accessible for Hg^{2+} capture. **(D)** Single-ion equilibrium adsorption by PAF-1-SH powder of Hg^{2+} and common ions in various water

sources (initial ion concentrations: 0.5 mM). The inset shows Hg^{2+} equilibrium adsorption by membranes in solutions with 100 ppm Hg^{2+} spiked in deionized water or common water supply sources. **(E)** Hg^{2+} recovery and adsorption performance of 20 wt% PAF-1-SH membranes regenerated using HCl and $NaNO_3$ (initial Hg^{2+} concentration: 100 ppm). All captured Hg^{2+} was desorbed and recovered. Minimal loss in target ion uptake is observed over 10 cycles. Error bars in each figure denote standard deviation ($n \geq 3$).

For use in an IC-ED process, adsorptive membranes must maintain high binding group accessibilities, uptake rates, selectivities, and regenerabilities. Batch adsorption experiments reveal that PAF membranes meet each performance standard. As high as 93% of PAF adsorption sites were found to remain accessible within a membrane matrix. Accessibility was calculated by comparing the measured Hg^{2+} equilibrium saturation capacity of 20 wt% PAF-1-SH membranes (318 mg g^{-1}, Fig. 2C) to their expected theoretical maximum capacity (see table S6 and fig. S23). Kinetic uptake measurements indicate that Hg^{2+} binding rates are nearly instantaneous in PAF-1-SH (fig. S26) and are rate-limited in PAF membranes by diffusion through the sPSF matrix rather than by binding to PAF-1-SH (fig. S27). PAF-1-SH as a bulk material exhibits exceptional selectivity for Hg^{2+} over a wide assortment of common competing ions in both single-component and complex multicomponent mixtures (Fig. 2D and fig. S28). This remarkable Hg^{2+} selectivity stems from optimal soft acid-soft base interactions between Hg^{2+} and thiol groups in PAF-1-SH (*17*) and, importantly, is preserved in PAF-1-SH-loaded membranes upon submersion in various practical source waters spiked with Hg^{2+} (Fig. 2D inset). Captured Hg^{2+} can be completely recovered upon exposure of Hg^{2+}-adsorbed PAF-1-SH membranes to concentrated HCl and 2 M $NaNO_3$ (Figure 2E). Notably, only an 8% loss in Hg^{2+} adsorption capacity is observed after 10 Hg^{2+} adsorption-desorption cycles of 20 wt% PAF-1-SH membranes, and the Hg^{2+} capacity remains approximately constant after three cycles.

To assess our proposed IC-ED process for treating practically any water source, 20 wt% PAF-1-SH membranes were tested for Hg^{2+}-capture electrodialysis of ~5 ppm Hg^{2+} spiked in synthetic groundwater, brackish water, and industrial wastewater (Fig. 3, A, B, and C). These complex feed water sources were chosen for their diversity of salinity levels, ion types, and pH (tables S4 and S5). In these proof-of-concept experiments, a custom-made two-compartment cell was used (figs. S30 to S32), with the membrane separating the feed from the "receiving" solution (10 mM HNO_3, to maintain conductivity and prevent metal precipitation). -4 V vs. Ag/AgCl were applied to drive feed cations through the membrane toward the receiving solution. Ion concentrations in both solutions were periodically measured. For each water source, Hg^{2+} was entirely captured by the adsorptive membranes, as Hg^{2+} was selectively reduced to concentrations below detection in the feed without permeating into the receiving solution. Meanwhile, all competing cations (Na^+, K^+, Mg^{2+}, Ca^{2+}, Ba^{2+}, Mn^{2+}, Fe^{3+}, Ni^{2+}, Cu^{2+}, Zn^{2+}, Cd^{2+}, Pb^{2+}) successfully transported into the receiving solution to achieve over 97-99% desalination of the feed. Remarkably, negligible amounts of each competing ion were captured by the membranes (figs. S37 to S43). No appreciable Hg^{2+} was captured when using neat sPSF membranes (figs. S34 to S36). These findings highlight the unique and extraordinarily selective multifunctional separation capabilities of an IC-ED method utilizing high-performance adsorptive membranes.

IC-ED breakthrough experiments reveal the outstanding target ion capture efficiency of IC-ED processes (Fig. 3D). Here, a feed containing a high Hg^{2+} concentration (~100 ppm) in a 0.1 M $NaNO_3$ supporting electrolyte was employed along with a 1 mM HNO_3 receiving solution. Hg^{2+} concentrations were periodically tracked to identify the "breakthrough time" at which Hg^{2+} was first detected in the receiving solution instead of captured in the membrane. As expected, Hg^{2+} immediately permeated through a neat sPSF membrane (Fig. 3D inset). Conversely, the breakthrough time by a 20 wt% PAF-1-SH membrane was approximately twice of that by a 10 wt% membrane, indicating high adsorbent utilization rates. To quantitatively evaluate the percentage of membrane-embedded adsorbents that are utilized before breakthrough in an IC-ED setup, the receiving Hg^{2+} concentrations were plotted against the amount of Hg^{2+} captured by PAFs in the membrane. Astonishingly, both the 10 wt% and 20 wt% PAF membranes experienced breakthrough after nearly all (97%) of the embedded adsorption sites were utilized. Utilization rates were calculated by comparing the Hg^{2+} capacity at breakthrough to the Hg^{2+} equilibrium capacity attained by accessible PAF-1-SH powder at approximately equivalent testing conditions (see fig. S28 and Supplementary Materials Section 1.9).

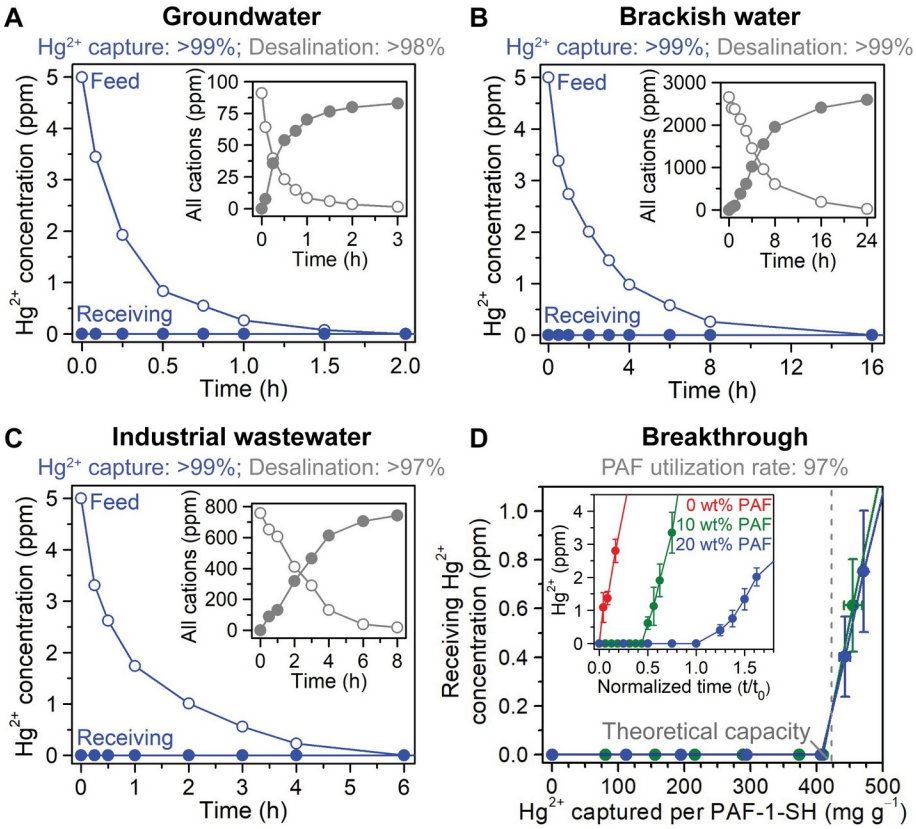

Fig. 3. IC-ED of diverse water sources. IC-ED by 20 wt% PAF-1-SH membranes of 5 ppm Hg^{2+} spiked in simulated **(A)** groundwater, **(B)** brackish water, and **(C)** industrial wastewater. All Hg^{2+} was selectively captured from the feeds (open circles) without detectable permeation into the receiving solutions (closed circles). (Insets) All other cations concurrently transported across the membranes to desalinate the feeds. -4 V vs. Ag/AgCl were applied. The long durations of the IC-ED tests are an artifact of the experimental setup rather than the materials or IC-ED method (see Supplementary Text). **(D)** IC-ED breakthrough. Receiving Hg^{2+} concentrations are plotted

against the amount of Hg^{2+} captured at different time intervals per gram of dry PAF-1-SH in 10 wt% (green) and 20 wt% (blue) PAF-1-SH membranes. The theoretical PAF-1-SH capacity (gray dotted line) corresponds to the Hg^{2+} uptake achieved by accessible PAF-1-SH powder at analogous testing conditions (see Supplementary Materials). (Inset) Receiving Hg^{2+} concentrations plotted against time normalized by the breakthrough time by a 20 wt% PAF-1-SH membrane (t_0, time when Hg^{2+} is detected in the receiving solution). Initial feed: 100 ppm Hg^{2+} in 0.1 M $NaNO_3$; applied voltage: -2 V vs. Ag/AgCl. Error bars denote the range of values measured over duplicate experiments.

We also show that IC-ED is a generalizable approach applicable for the recovery of any target ion, provided that an adsorbent selective for the target ion exists. This generalizability allows IC-ED processes to be designed according to whatever target ions are present in desired feed water sources. To validate this versatility, we tuned the ion selectivity of sPSF composite membranes by incorporating other PAF adsorbents highly selective for other common waterborne contaminants (PAF-1-SMe for Cu^{2+} (*19*) and PAF-1-ET for Fe^{3+} (*24*), see Supplementary Materials). Notably, membranes embedded with these PAFs each feature excellent optical transparency (fig. S4), flexibility (fig. S5), dispersibility (figs. S16 and S19), and polymer matrix compatibility (fig. S19 and table S3), indicating that a multitude of PAFs can be easily incorporated into ion exchange or water treatment membranes. Membranes composed 20 wt% of PAF-1-SMe or PAF-1-ET were then tested in our IC-ED setup. Feed solutions consisted of 6 ppm Cu^{2+} or 2.3 ppm Fe^{3+}, respectively, in 0.1 M HEPES buffer (to supply competing ions and prevent precipitation upon OH^- generation). Excitingly, both membranes selectively captured their respective target ions without capturing competing ions, as feed concentrations of each target ion were reduced below detection without permeation into the receiving solutions (Fig. 4, A and B). Reusable water was simultaneously produced as the membranes achieved >96% desalination of the feeds. Negligible target ion capture was obtained when neat sPSF membranes were tested (figs. S47 and S48).

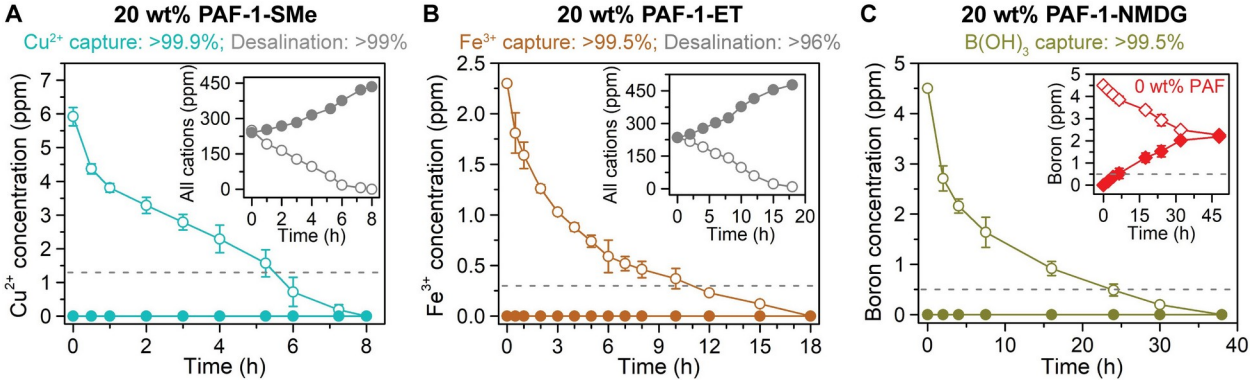

Fig. 4. Tuning membranes to selectively recover various target solutes. (A) Cu^{2+}- and **(B)** Fe^{3+}-capture electrodialysis (applied voltages: -2 V and -1.5 V vs. Ag/AgCl, respectively) using membranes composed 20 wt% of the Cu^{2+}-selective PAF-1-SMe or the Fe^{3+}-selective PAF-1-ET, respectively. HEPES buffer (0.1 M) was used as the source water in each solution to supply competing ions and maintain constant pH. (Insets) All competing cations transport across the membrane to desalinate the feed. **(C)** $B(OH)_3$-capture diffusion dialysis of groundwater containing 4.5 ppm boron using membranes comprised 20 wt% of the $B(OH)_3$-selective PAF-1-

NMDG or (inset) using neat sPSF membranes for comparison. No voltage was applied. Error bars in each figure denote the range of values measured over duplicate experiments. Gray dotted lines indicate recommended maximum contaminant limits imposed for each contaminant in water (guidelines: U.S. Environmental Protection Agency (EPA) for Cu^{2+} (*29*), U.S. EPA and World Health Organization for Fe^{3+} (*29, 30*), agricultural restrictions for sensitive crops for $B(OH)_3$ (*31*)). Open and closed circles denote feed and receiving concentrations, respectively.

Finally, fundamentals uncovered in our IC-ED analyses can also be applied broadly to create other new multifunctional membrane processes. To this end, we tuned membranes to contain the $B(OH)_3$-selective adsorbent PAF-1-NMDG (*23*) and developed a solute-capture diffusion dialysis (SC-DD) process with $B(OH)_3$ as the target solute. In this process, concentration gradients, rather than electric potential gradients, drive solute transport across the membrane. Membranes composed 20 wt% of PAF-1-NMDG in sPSF were placed in a diffusion dialysis setup (fig. S33). Synthetic groundwater with 4.5 ppm $B(OH)_3$ was inserted into the feed half-cell, while the receiving half-cell was charged with deionized water. To our excitement, the 20 wt% PAF-1-NMDG membranes selectively captured $B(OH)_3$ as it transported through the membrane, as $B(OH)_3$ was reduced to concentrations below detection in the feed without any measured permeation into the receiving solution (Fig. 4C). No appreciable $B(OH)_3$ was captured when a conventional neat sPSF membrane was used (Fig. 4C inset). Membranes tuned with Hg^{2+}-selective PAF-1-SH likewise exhibited selective Hg^{2+} capture when employed in a SC-DD setup (fig. S52). These results indicate that a wide array of efficient multifunctional processes like IC-ED and SC-DD can be developed through the modification of traditional membrane processes, regardless of the transport driving force required.

In conclusion, to the best of our knowledge, we report the first one-step process that can desalinate water for re-use and concurrently recover ions of interest selectively. We also report the first water treatment and ion exchange mixed matrix membranes incorporated with PAFs. This new class of composites exhibits excellent dispersibility, compatibility, stability, and tunability. Furthermore, we showed the high efficiency and versatility of an IC-ED strategy through adsorption and electrodialysis studies using diverse source waters (groundwater, brackish water, industrial wastewater, seawater) and common target contaminants (Hg^{2+}, Cu^{2+}, Fe^{3+}, $B(OH)_3$). As validated by SC-DD, IC-ED principles developed in this report can also be applied widely to originate efficient multifunctional processes stemming from practically any traditional membrane process. For example, adsorbent-embedded membranes may be used to supplant traditional membranes used in gas separations, direct air capture, blood dialysis, organic solvent nanofiltration, and fuel cell operations to simultaneously achieve traditional membrane operations while selectively capturing contaminants like Hg, CO_2, blood toxins, and CO. We have begun to investigate these promising possibilities and to devise other new classes of exceptionally selective and tunable adsorptive composites.

References and Notes:

1. M. M. Mekonnen, A. Y. Hoekstra, Four billion people facing severe water scarcity. *Sci. Adv.* **2**, e1500323 (2016).
2. M. A. Shannon, P. W. Bohn, M. Elimelech, J. G. Georgiadis, B. J. Mariñas, A. M. Mayes, Science and technology for water purification in the coming decades. *Nature* **452**, 301-310 (2008).

3. J. R. Werber, C. O. Osuji, M. Elimelech, Materials for next-generation desalination and water purification membranes. *Nat. Rev. Mater.* **1**, 16018 (2016).
4. M. R. Landsman, R. Sujanani, S. H. Brodfuehrer, C. M. Cooper, A. G. Darr, R. J. Davis, K. Kim, S. Kum, L. K. Nalley, S. M. Nomaan, C. P. Oden, A. Paspureddi, K. K. Reimund, L. S. Rowles, S. Yeo, D. F. Lawler, B. D. Freeman, L. E. Katz, Water treatment: Are membranes the panacea? *Annu. Rev. Chem. Biomol. Eng.* **11**, 559-585 (2020).
5. D. S. Sholl, R. P. Lively, Seven chemical separations to change the world. *Nature* **532**, 435-437 (2016).
6. W. W. Li, H. Q. Yu, B. E. Rittmann, Chemistry: Reuse water pollutants. *Nature* **528**, 29-31 (2015).
7. H. B. Park, J. Kamcev, L. M. Robeson, M. Elimelech, B. D. Freeman, Maximizing the right stuff: The trade-off between membrane permeability and selectivity. *Science* **356**, eaab0530 (2017).
8. J. R. Werber, A. Deshmukh, M. Elimelech, The critical need for increased selectivity, not increased water permeability, for desalination membranes. *Environ. Sci. Technol. Lett.* **3**, 112-120 (2016).
9. M. Elimelech, W. A. Phillip, The future of seawater desalination: Energy, technology, and the environment. *Science* **333**, 712-717 (2011).
10. S. Bolisetty, R. Mezzenga, Amyloid-carbon hybrid membranes for universal water purification. *Nat. Nanotechnol.* **11**, 365-371 (2016).
11. Y. Zhang, J. R. Vallin, J. K. Sahoo, F. Gao, B. W. Boudouris, M. J. Webber, W. A. Phillip, High-affinity detection and capture of heavy metal contaminants using block polymer composite membranes. *ACS Cent. Sci.* **4**, 1697-1707 (2018).
12. K. V. Petrov, L. Paltrinieri, L. Poltorak, L. de Smet, E. J. R. Sudholter, Modified cation-exchange membrane for phosphate recovery in an electrochemically assisted adsorption-desorption process. *Chem. Commun.* **56**, 5046-5049 (2020).
13. S. Chaudhury, O. Nir, Electro-enhanced membrane sorption: A new approach for selective ion separation and its application to phosphate and arsenic removal. *Ind. Eng. Chem. Res.* **59**, 10595-10605 (2020).
14. J. E. Bachman, Z. P. Smith, T. Li, T. Xu, J. R. Long, Enhanced ethylene separation and plasticization resistance in polymer membranes incorporating metal-organic framework nanocrystals. *Nat. Mater.* **15**, 845-849 (2016).
15. T. Ben, H. Ren, S. Ma, D. Cao, J. Lan, X. Jing, W. Wang, J. Xu, F. Deng, J. M. Simmons, S. Qiu, G. Zhu, Targeted synthesis of a porous aromatic framework with high stability and exceptionally high surface area. *Angew. Chem. Int. Ed.* **48**, 9457-9460 (2009).
16. Y. Tian, G. Zhu, Porous aromatic frameworks (PAFs). *Chem. Rev.* **120**, 8934-8986 (2020).
17. B. Li, Y. Zhang, D. Ma, Z. Shi, S. Ma, Mercury nano-trap for effective and efficient removal of mercury(II) from aqueous solution. *Nat. Commun.* **5**, 5537 (2014).
18. S. Demir, N. K. Brune, J. F. Van Humbeck, J. A. Mason, T. V. Plakhova, S. Wang, G. Tian, S. G. Minasian, T. Tyliszczak, T. Yaita, T. Kobayashi, S. N. Kalmykov, H. Shiwaku, D. K. Shuh, J. R. Long, Extraction of lanthanide and actinide ions from

aqueous mixtures using a carboxylic acid-functionalized porous aromatic framework. *ACS Cent. Sci.* **2**, 253-265 (2016).
19. S. Lee, G. Barin, C. M. Ackerman, A. Muchenditsi, J. Xu, J. A. Reimer, S. Lutsenko, J. R. Long, C. J. Chang, Copper capture in a thioether-functionalized porous polymer applied to the detection of Wilson's Disease. *J. Am. Chem. Soc.* **138**, 7603-7609 (2016).
20. Y. J. Yang, Z. J. Yan, L. L. Wang, Q. H. Meng, Y. Yuan, G. S. Zhu, Constructing synergistic groups in porous aromatic frameworks for the selective removal and recovery of lead(II) ions. *J. Mater. Chem. A* **6**, 5202-5207 (2018).
21. Y. Yuan, Y. Yang, X. Ma, Q. Meng, L. Wang, S. Zhao, G. Zhu, Molecularly imprinted porous aromatic frameworks and their composite components for selective extraction of uranium ions. *Adv. Mater.* **30**, 1706507 (2018).
22. B. Li, Q. Sun, Y. Zhang, C. W. Abney, B. Aguila, W. Lin, S. Ma, Functionalized porous aromatic framework for efficient uranium adsorption from aqueous solutions. *ACS Appl. Mater. Interfaces* **9**, 12511-12517 (2017).
23. J. Kamcev, M. K. Taylor, D. M. Shin, N. N. Jarenwattananon, K. A. Colwell, J. R. Long, Functionalized porous aromatic frameworks as high-performance adsorbents for the rapid removal of boric acid from water. *Adv. Mater.* **31**, 1808027 (2019).
24. S. Lee, A. Uliana, M. K. Taylor, K. Chakarawet, S. R. S. Bandaru, S. Gul, J. Xu, C. M. Ackerman, R. Chatterjee, H. Furukawa, J. A. Reimer, J. Yano, A. Gadgil, G. J. Long, F. Grandjean, J. R. Long, C. J. Chang, Iron detection and remediation with a functionalized porous polymer applied to environmental water samples. *Chem. Sci.* **10**, 6651-6660 (2019).
25. T. T. Ma, R. Zhao, Z. N. Li, X. F. Jing, M. Faheem, J. Song, Y. Y. Tian, X. J. Lv, Q. H. Shu, G. S. Zhu, Efficient gold recovery from e-waste via a chelate-containing porous aromatic framework. *ACS Appl. Mater. Interfaces* **12**, 30474-30482 (2020).
26. X. Li, Y. Liu, J. Wang, J. Gascon, J. Li, B. Van der Bruggen, Metal-organic frameworks based membranes for liquid separation. *Chem. Soc. Rev.* **46**, 7124-7144 (2017).
27. S. J. D. Smith, R. Hou, K. Konstas, A. Akram, C. H. Lau, M. R. Hill, Control of physical aging in super-glassy polymer mixed matrix membranes. *Acc. Chem. Res.* **53**, 1381-1388 (2020).
28. H. Fan, N. Y. Yip, Elucidating conductivity-permselectivity tradeoffs in electrodialysis and reverse electrodialysis by structure-property analysis of ion-exchange membranes. *J. Membr. Sci.* **573**, 668-681 (2019).
29. United States Environmental Protection Agency, "2018 edition of the drinking water standards and health advisories," (U.S. EPA, Washington, DC, 2018).
30. World Health Organization, "Guidelines for drinking-water quality, 4th edition, incorporating the 1st addendum," (WHO, Geneva, 2017).
31. E. Guler, C. Kaya, N. Kabay, M. Arda, Boron removal from seawater: State-of-the-art review. *Desalination* **356**, 85-93 (2015).

Acknowledgments: We thank Dr. Hiroyasu Furukawa for analysis of pore size distributions, Dr. Ting Xu for assistance with dynamic light scattering measurements, Dr. Nitash P. Balsara for potentiostat use, Jim Breen for fabrication of electrodialysis cells, Dr. Daniel J. Miller for assistance with water contact angle measurements, Dr. Katie R. Meihaus for editorial assistance, and Dr. Robert Kostecki, Dr. Sumin Lee, and Ever Velasquez for helpful discussions. **Funding:** This research was supported by the Center for Gas Separations Relevant to Clean Energy

Technologies, an Energy Frontier Research Center supported by the U.S. Department of Energy, Office of Science, Office of Basic Energy Sciences, under Award DE-SC0001015. Preliminary electrodialysis experiments and the design of electrodialysis cells were also partially supported by the Laboratory Directed Research and Development (LDRD) Program under U.S. Department of Energy Contract LB18010. The U.S. National Science Foundation is thanked for providing graduate fellowship support for A.A.U. and M.K.T. **Author contributions:** A.A.U., J.J.U., and J.R.L. formulated the project with valuable input from N.B., J.K., and M.K.T. A.A.U. synthesized the porous aromatic frameworks and membranes with assistance from J.K. and M.K.T. A.A.U. performed and analyzed all material characterizations. A.A.U. collected and analyzed the adsorption data. A.A.U. and N.B. designed the electrodialysis cells. A.A.U. collected and analyzed the electrodialysis and diffusion dialysis data, while N.B. performed preliminary electrodialysis experiments. A.A.U. and J.R.L. wrote the manuscript, and all authors contributed to revising the manuscript. **Competing interests:** The authors declare the following competing interests: the University of California, Berkeley has applied for a patent on some of the technology discussed herein, on which A.A.U., N.B., J.J.U., and J.R.L. are listed as co-inventors, as well as an additional patent on some of the materials discussed herein, on which A.A.U. and J.R.L. are listed as co-inventors. **Data and materials availability:** All data are available in the main text or the supplementary materials.

Supplementary Materials:

Materials and Methods

Figures S1-S53

Tables S1-S7

References (*32-55*)